Available online at www.sciencedirect.com
SCIENCE DIRECT®
Inorganica Chimica Acta 357 (2004) 3943–3949
Inorganica Chimica Acta
www.elsevier.com/locate/ica

Coordination behavior of phosphino-phosphaferrocenes: monodentate versus bidentate coordination to divalent palladium ☆

Masamichi Ogasawara [a,*], Yonghui Ge [a], Kiyohiko Nakajima [b], Tamotsu Takahashi [a,*]

[a] *Catalysis Research Center and Graduate School of Pharmaceutical Sciences, Hokkaido University, and SORST, Japan Science and Technology Corporation (JST), Kita-ku, Sapporo 001-0021, Japan*
[b] *Department of Chemistry, Aichi University of Education, Igaya, Kariya, Aichi, 448-8542, Japan*

Received 9 April 2004; accepted 1 May 2004
Available online 8 June 2004

Dedicated to Professor Tobin J. Marks on the occasion of his 60th birthday

Abstract

Two novel phosphino-phosphaferrocenes [η^5-$C_5H_4(CH_2)_nPPh_2$]Fe(η^5-PC_4H_2-2,5-Cy_2) (**PP1**: $n = 1$; **PP2**: $n = 2$) have been designed and prepared in order to clarify weak chelate effect in the previously reported (η^5-$C_5H_4CH_2PPh_2$)Fe[η^5-PC_4H_2-2,5-((–)-menthyl)$_2$] (**1**). ^{31}P NMR studies of reactions of **PP1** with $PdCl_2$(cod) (**6**) revealed that **PP1** showed stronger tendency to coordinate to the Pd^{II} center in bidentate fashion compared to **1**. On the other hand, chelate effect in **PP2** was negligibly weak and a reaction of **PP2** with **6** in a **PP2/6** = 2/1 molar ratio gave a complex $PdCl_2$(**PP2**)$_2$ (**10**) cleanly in which **PP2** coordinated to the palladium center at the PPh_2 moiety as a monodentate ligand. X-ray crystal structure studies of chelate complexes $PdCl_2$(**PP1**) (**7**) and $PdCl_2$(**PP2**) (**9**) showed that **9** had deviations from an idealized geometry in the square planar complex which could be attributed to a larger chelate ring of **PP2**, while **PP1** in **7** constructed nearly ideal geometry for the square planar complex.

From comparison of the coordination behavior between **1**, **PP1**, and **PP2**, it is concluded that steric bulk of (–)-menthyl groups in **1** is the main factor of the weak chelate coordination of **1**.

Keywords: Phosphaferrocene; Phosphine; Palladium(II); Chelate effect

1. Introduction

Recently, we have reported preparation of a novel chiral phosphino-phosphaferrocene **1** and its application to palladium-catalyzed asymmetric allylic alkylation [1]. The ligand **1** showed excellent performance in the asymmetric reaction (up to 99% ee with nearly quantitative yield) under carefully controlled reaction conditions; appropriate molar ratio between Pd and the chiral ligand was especially important for achieving the high-level of enantioselectivity. The ligand **1** shows two distinctive coordination modes depending on stoichiometry between **1** and Pd^{II}. While the ligand **1** forms a chelate complex in the presence of more than 1 equiv of a $PdCl_2$ precursor ($[\mathbf{1}]/[Pd^{II}] < 1$), it has the tendency to dissociate its chiral phosphaferrocene moiety from the divalent palladium acting as a monodentate ligand in the presence of less than 1 equiv of $PdCl_2$ ($[\mathbf{1}]/[Pd^{II}] > 1$). The two coordination modes are reversible and conversion between the two is spontaneous and clean. With a molar ratio of $\mathbf{1}/Pd^{II} = 2/1$, *cis*- and *trans*-$PdCl_2(\mathbf{1})_2$, where **1** was coordinating to the palladium center in the monodentate fashion at the PPh_2 group, are only observable species and no complex with chelating **1** and no free ligand **1** were detected. These observations suggest

☆ Supplementary data associated with this article can be found, in the online version, at doi:10.1016/j.ica.2004.05.019.

* Corresponding authors. Tel.: +81-11-706-9154; fax: +81-11-706-9150 (M. Ogasawara), Tel.: +81-11-706-9149; fax: +81-11-706-9150 (T. Takahashi).

0020-1693/$ - see front matter © 2004 Elsevier B.V. All rights reserved.
doi:10.1016/j.ica.2004.05.019

that coordination ability between the two donors in **1** is very different, and thus virtually no chelate effect was seen in **1**.

On the other hand, the coordination behavior of other known phosphino-phosphaferrocenes, such as **2** [2] and **3** [3] reported by Ganter and Fu, respectively, is different from that of **1**. Although phosphaferrocenes are known to be weaker σ-donors than classical tertiary phosphines [4], the α-(diphenylphosphinomethyl)phosphaferrocenes **2** and **3** showed persistent bidentate coordination to transition metals. Chelate effect overcomes the electronic inferiority of the phosphaferrocene moieties in **2** and **3**, however, a similar chelate effect seems not to be a dominant factor regulating the coordination modes of **1** as described above [1]. The latter fact may be the limitation of **1** on its application to metal-catalyzed asymmetric reactions as a chiral ligand. Because in the monodentate coordination of **1**, the chiral groups are far apart from the Pd center, and thus the ability of **1** as an asymmetric chiral ligand is diminished.

Based on this background, we have intended to clarify the origin of the distinctive coordination behavior of **1**. Here are the results to this goal.

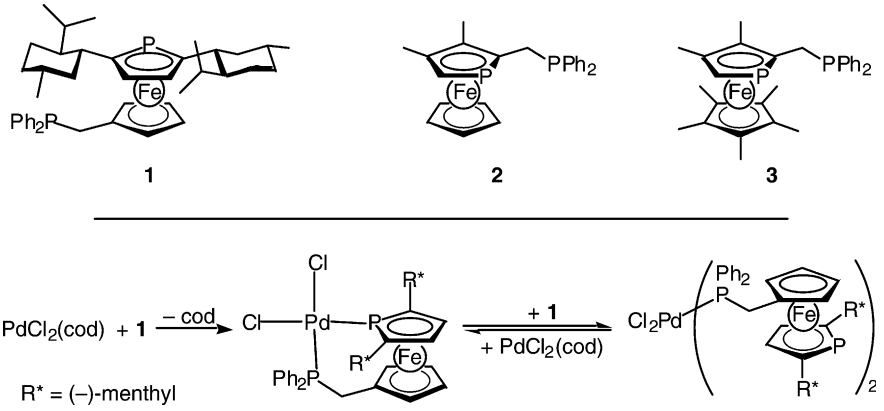

2. Experimental

2.1. General procedures

All anaerobic and/or moisture sensitive manipulations were carried out with standard Schlenk techniques under predried nitrogen or with glovebox techniques under prepurified argon. Tetrahydrofuran, Et_2O, and 1,4-dioxane were distilled from benzophenone-ketyl under nitrogen prior to use. Dichloromethane was distilled from CaH_2 under nitrogen prior to use. EtOH was dried over magnesium ethoxide, distilled, and stored in a glass flask with a Teflon stopcock under nitrogen. $CDCl_3$ was dried over P_2O_5, degased by three freeze–pump–thaw cycles, and vacuum-transferred. $FcCH_2CH_2Br$ (Fc = ferrocenyl) [5], [(η^6-mesitylene)Fe(η^5-$C_5H_4CH_2PPh_2$)]PF_6 (**4**) [1], 2,5-dicyclohexyl-1-phenylphosphole [6], and $PdCl_2$(cod) [7] were prepared as reported. All the other reagents were obtained from commercial sources and used as received. NMR spectra were recorded on a JEOL JNM-AL300 spectrometer (^{1}H, 300 MHz; ^{13}C, 75 MHz; ^{31}P, 121 MHz). ^{1}H and ^{13}C chemical shifts are reported in ppm downfield of internal tetramethylsilane. ^{31}P NMR chemical shifts are externally referenced to 85% H_3PO_4.

2.2. [2-(Diphenylphosphino)ethyl]ferrocene

To a solution of $FcCH_2CH_2MgBr$, which was prepared from $FcCH_2CH_2Br$ (8.14 g, 27.8 mmol) and Mg (730 mg, 30.0 mmol) in THF (50 mL), was added a THF (20 mL) solution of Ph_2PCl (6.34 g, 28.7 mmol) dropwise at 0 °C. After stirring the mixture for 3 h at room temperature, all the volatiles were evaporated to dryness under reduced pressure. The residue was extracted with benzene, then the evaporated extract was purified by column chromatography over silica gel (elution with hexane/benzene = 3/1) under nitrogen. Yield: 7.86 g (19.7 mmol, 71%). This material was >95% pure (by ^{1}H and ^{31}P NMR analyses) and used for the following step without further purification. ^{1}H NMR ($CDCl_3$): δ 2.26–2.30 (m, 2H), 2.42–2.47 (m, 2H), 4.03–4.05 (m, 2H), 4.04 (s, 5H), 4.06–4.07 (m, 2H), 7.32–7.36 (m, 6H), 7.43–7.46 (m, 4H). ^{13}C{^{1}H} NMR ($CDCl_3$): δ 25.92 (d, J_{PC} = 19.1 Hz), 29.31 (d, J_{PC} = 11.4 Hz), 67.24 (s), 67.80 (s), 68.49 (s), 89.51 (d, J_{PC} = 15.5 Hz), 128.50 (d, J_{PC} = 6.7 Hz),128.66 (s), 132.74 (d, J_{PC} = 18.1 Hz), 138.54 (d, J_{PC} = 12.4 Hz). ^{31}P{^{1}H} NMR ($CDCl_3$): δ −15.0 (s).

2.3. (η^6-Mesitylene) [η^5-(2-(diphenylphosphino)ethyl) cyclopentadienyl]iron(II) hexafluorophosphate (**5**)

Aluminum chloride (6.40 g, 48.0 mmol), aluminum powder (324 mg, 12.0 mmol), $FcCH_2CH_2PPh_2$ (4.23 g, 11.0 mmol), mesitylene (6.30 mL, 45.0 mmol), and water

(0.22 mL, 12 mmol) were refluxed in cyclohexane (35 mL) for 5 h. The mixture was cooled to 0 °C and quenched with cold water (40 mL). The aqueous layer was separated, filtered, and washed with ether. Excess NH_4PF_6 solution was added and the resulting yellow solid was collected on a filter and washed with cold water. The solid was dried, washed with ether, and recrystallized from CH_2Cl_2/ether to give the title compound with ca. 33% of inseparable [(η^6-mesitylene)FeCp]PF_6. Yield: 4.53 g (ca. 48% of **7** and 24% of [($C_6H_3Me_3$)FeCp]PF_6). ^{1}H NMR (acetone-d_6): δ 2.32 (br, 13H), 4.83–4.86 (m, 4H), 5.96 (s, 3H), 7.17–7.52 (m, 10H). $^{31}P\{^1H\}$ NMR (acetone-d_6; −25 °C): δ −6.5 (br), 69.7 (m).

2.4. 1′-(Diphenylphosphinomethyl)-2,5-dicyclohexyl-1-phosphaferrocene (*PP1*)

Lithium metal (230 mg, 33.1 mmol) was added to a solution of 2,5-dicyclohexyl-1-phenylphosphole (900 mg, 2.77 mmol) in dioxane (40 mL) at room temperature. The mixture was stirred at 40 °C until disappearance of the phosphole (checked by TLC). The mixture was added to a solution of **4** (3.10 g, ca. 92% purity, ca. 4.88 mmol) in 1,4-dioxane (75 mL) at 100 °C. The resulting mixture was stirred for 2 h at this temperature. After cooling, ca. 60 mL of benzene was added and the solution was filtered through a pad of Celite. The mixture was evaporated to dryness under reduced pressure and the crude product was chromatographed on silica gel twice (first elution with hexane/toluene = 4/1, second elution with hexane/CH_2Cl_2 = 10/1) under nitrogen. Yield: 164 mg (0.289 mmol, 10%). ^{1}H NMR ($CDCl_3$): δ 1.01–1.27 (m, 10H), 1.63–2.02 (m, 12H), 3.19 (s, 2H), 3.76 (m, 2H), 4.14 (m, 2H), 4.84 (d, J_{PH} = 5.0 Hz, 2H), 7.31–7.42 (m, 10H). $^{31}P\{^1H\}$ NMR ($CDCl_3$): δ −74.7 (s), −12.8 (s). *Anal*. Calc. for $C_{34}H_{42}FeP_2$: C, 72.09; H, 7.12. Found: C, 72.46; H, 7.41%.

2.5. 1′-[2-(Diphenylphosphino)ethyl]-2,5-dicyclohexyl-1-phosphaferrocene (*PP2*)

Lithium metal (210 mg, 30.3 mmol) was added to a solution of 2,5-dicyclohexyl-1-phenylphosphole (800 mg, 2.46 mmol) in dioxane (40 mL) at room temperature. The mixture was stirred at 40 °C until disappearance of the phosphole (checked by TLC). The mixture was added to a solution of **5** (2.60 g, ca. 67% purity, ca. 3.28 mmol) in 1,4-dioxane (50 mL) at 100 °C. The resulting mixture was stirred for 2 h at this temperature. After cooling, ca. 60 mL of benzene was added and the solution was filtered through a pad of Celite. The mixture was evaporated to dryness under reduced pressure and the crude product was chromatographed on silica gel (elution with hexane/toluene = 4/1) under nitrogen. Yield: 791 mg (1.36 mmol, 55%). ^{1}H NMR ($CDCl_3$): δ 0.92–1.21 (m, 10H), 1.55–1.90 (m, 12H), 2.23–2.29 (m, 2H), 2.37–2.45 (m, 2H), 3.85 (m, 2H), 4.15 (m, 2H), 4.69 (d, J_{PH} = 4.6 Hz, 2H), 7.26–7.42 (m, 10H). $^{31}P\{^1H\}$ NMR ($CDCl_3$): δ −75.4 (s), −16.7 (s). *Anal*. Calc. for $C_{35}H_{42}FeP_2$: C, 72.42; H, 7.29. Found: C, 72.36; H, 7.27%.

2.6. Dichloro[1′-(diphenylphosphinomethyl)-2,5-dicyclohexyl-1-phosphaferrocene]palladium(II) (*7*)

An equimolar mixture of $PdCl_2$(cod) and **PP1** in dichloromethane was stirred for 30 min at room temperature and then all the volatiles were removed under reduced pressure. The yellow residue was dissolved in a minimum amount of CH_2Cl_2. Recrystallization by slow diffusion of pentane into the CH_2Cl_2 solution at room temperature gave the title complex quantitatively as orange crystals. ^{1}H NMR ($CDCl_3$): δ 0.97–1.80 (m, 20H), 2.07 (br d, J_{PH} = 12.1 Hz, 2H), 3.03 (dd, J_{PH} = 9.9 and 5.9 Hz, 2H), 3.31 (br, 2H), 4.38 (br, 2H), 4.85 (d, J_{PH} = 20.9 Hz, 2H), 7.50–7.55 (m, 6H), 7.83–7.90 (m, 4H). $^{31}P\{^1H\}$ NMR ($CDCl_3$): δ 32.4 (d, J_{PP} = 9.9 Hz, 1P), 66.9 (d, J_{PP} = 9.9 Hz, 1P). *Anal*. Calc. for $C_{34}H_{40}Cl_2FeP_2Pd$: C, 54.90; H, 5.42. Found: C, 54.69; H, 5.67%.

2.7. Dichloro[1′-[2-(diphenylphosphino)ethyl]-2,5-dicylohexyl-1-phosphaferrocene]palladium(II) (*9*)

This complex was prepared in quantitative yield by the analogous method used for the synthesis of **7**. ^{1}H NMR ($CDCl_3$): δ 1.18–1.30 (m, 6H), 1.44–2.13 (m, 16H), 2.71–2.80 (m, 2H), 2.91–3.00 (m, 2H), 3.92 (br, 2H), 4.45 (m, 2H), 5.05 (d, J_{PH} = 19.4 Hz, 2H), 7.47–7.58 (m, 6H), 7.97 (br, 4H). $^{31}P\{^1H\}$ NMR ($CDCl_3$): δ 20.1 (d, J_{PP} = 12.2 Hz, 1P), 20.8 (d, J_{PP} = 12.2 Hz, 1P). *Anal*. Calc. for $C_{35}H_{42}Cl_2FeP_2Pd$: C, 55.47; H, 5.59. Found: C, 55.31; H, 5.68%.

3. Results and discussion

3.1. Design and preparation of novel phosphino-phosphaferrocenes

Two steric factors, which might restrict chelate coordination of **1**, were examined; one is steric congestion at the phosphorus atom in the phosphaferrocene moiety, the other is strain in the chelate ring. For this purpose, two novel phosphino-phosphaferrocene ligands **PP1** and **PP2** were designed and prepared (Scheme 1). The ligand **PP1** has two cyclohexyl groups at the α- and α′-positions of the phospholyl in place of two (–)-menthyl groups in **1**. The smaller cyclohexyl substituents would reduce steric congestion at the phospholyl moiety in **1** without changing the electronic properties of it. The compound **PP2** has an additional CH_2 unit between the

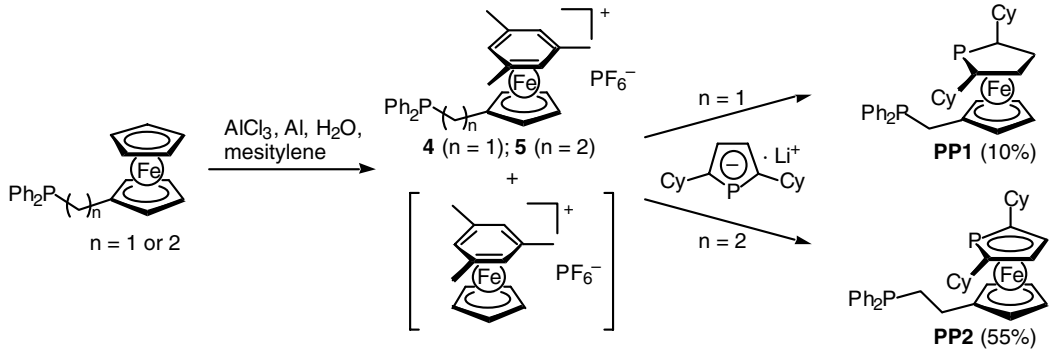

Scheme 1.

phosphaferrocenyl and diphenylphosphino groups compared to **1** as well as **PP1**, which allow more flexible coordination of **PP2** and may reduce the strain of the chelate if it existed.

The phosphino-phosphaferrocenes **PP1** and **PP2** were prepared by an analogous method used for the synthesis of **1** as outlined in Scheme 1 [8]. Reaction of lithium 2,5-dicyclohexylphospholide with a cationic (η^6-mesitylene)Fe(II) complex **4** or **5** [9], which were prepared from the corresponding [ω-(diphenylphosphino)alkyl]ferrocene as an inseparable mixture with [(η^6-mesitylene)FeCp]PF_6, and subsequent purification by column chromatography over silica gel gave the phosphino-phosphaferrocene **PP1** (10%) or **PP2** (55%). In the ^{31}P NMR spectra of **PP1** or **PP2**, signals for the phosphaferrocene moieties are detected in the high field region (δ −74.7 for **PP1**; δ −75.4 for **PP2** in $CDCl_3$), while those of the –PPh_2 are seen in the relatively lower field region (δ −12.8 for **PP1**; δ −16.7 for **PP2** in $CDCl_3$). No coupling is detected between the two ^{31}P signals in **PP1** or **PP2**.

3.2. Coordination behavior of the phosphino-phosphaferrocene

Reactions of **PP1** with $PdCl_2$(cod) (**6**) in $CDCl_3$ were examined in various **PP1/6** molar ratios. The coordination behavior of **PP1** was monitored by $^{31}P\{^1H\}$ NMR (Fig. 1). Treatment of **PP1** with an equimolar of **6** completely consumed the phosphino-phosphaferrocene to give a new Pd complex $PdCl_2$(**PP1**) (**7**) cleanly, in which **PP1** coordinated in a chelating fashion (Scheme 2). The two ^{31}P NMR resonances of **7**, detected at δ 32.4 (–PPh_2) and 66.9 (phosphaferrocene), coupled to each other with a small coupling constant ($^2J_{PP}$ = 9.9 Hz). This indicates the coordination of **PP1** in a *cis* fashion as expected.

With a molar ratio of **PP1/6** = 2/1, a new species, which was assigned to *cis*-**8**, was detected in the ^{31}P NMR spectrum in addition to the complex **7** (Scheme 2). The existence of the chelate complex **7** with the **PP1/6** = 2/1 molar ratio indicated that certain chelate effects were operative between **PP1** and the $Pd^{II}Cl_2$ fragment, which was different from the coordination behavior of **1** (vide supra) [1]. The effective chelate effect of **PP1** could be ascribed to the sterically less crowded phospholyl in **PP1** than that in **1**. Signals for the free **PP1** were not clearly recognized for this sample at room temperature, however, very broad resonances were seen at ca. δ 20 and δ −75. This could be explained as a rapid

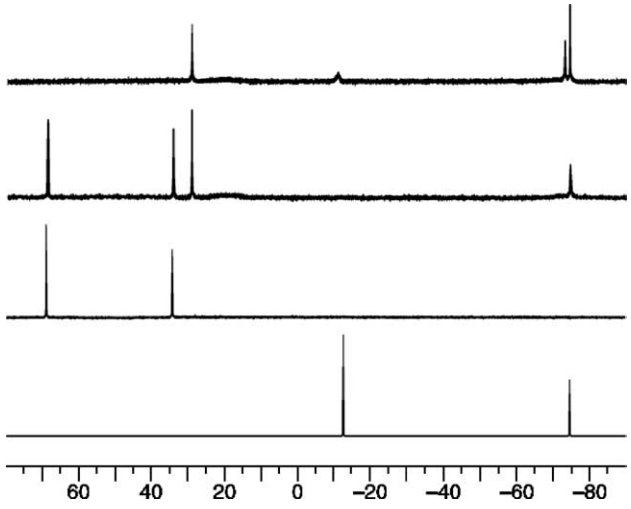

Fig. 1. $^{31}P\{^1H\}$ NMR spectra of reaction mixture of **PP1** and **6** with varied molar ratios (from bottom to top, **PP1/6** = 1/0, 1/1, 2/1, 3/1) recorded at 121 MHz in $CDCl_3$.

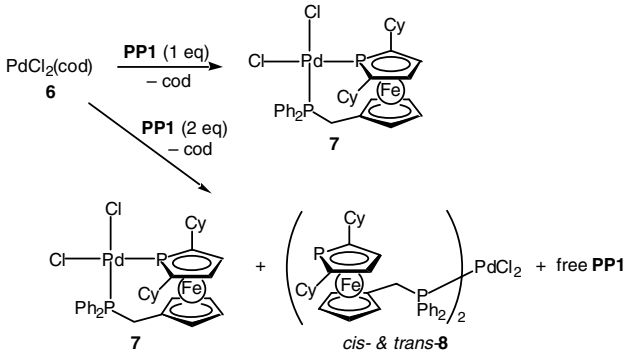

Scheme 2.

phosphine exchange between *trans*-**8** and **PP1**. The Pd-PPh_2 bond in *trans*-**8** is relatively weaker than that in *cis*-**8** because of the stronger *trans* effect of the PPh_2 group compared to that of Cl [10]. And thus, the remaining free **PP1** preferentially exchanges with the coordinating **PP1** in *trans*-**8**.

With a large excess of **PP1** (ca. 3 equiv to **6**), *cis*-**8** and broad signals at δ −12.7 and δ −74.5 (assignable to the exchanging free **PP1** and *trans*-**8**) were observed, but no **7** was detected. All these processes are reversible and addition of **6** to the mixture of *cis*- and *trans*-**8** regenerates **7** quantitatively.

The reactions between **PP2** and **6** are much simple (Fig. 2 and Scheme 3). The phosphino-phosphaferrocene **PP2** forms a chelate complex **9** with molar ratios of **PP2/6** $\leqslant$ 1. In the presence of more than equimolar of **PP2** to **6**, the phosphaferrocene moiety in **9** cleanly replaced with

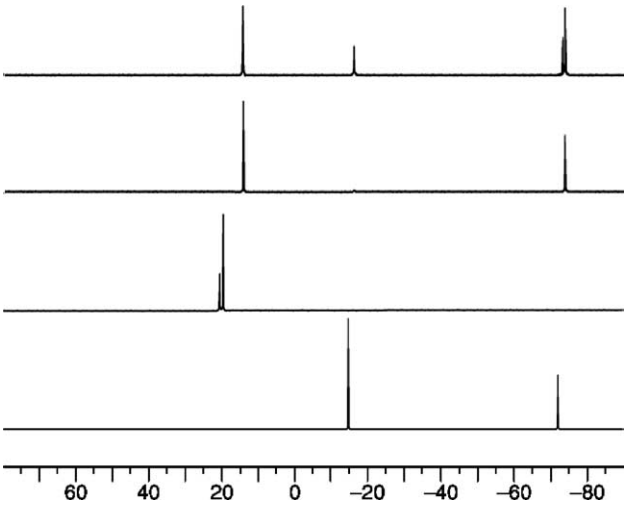

Fig. 2. $^{31}P\{^1H\}$ NMR spectra of reaction mixture of **PP2** and **6** with varied molar ratios (from bottom to top, **PP2/6** = 1/0, 1/1, 2/1, 3/1) recorded at 121 MHz in $CDCl_3$.

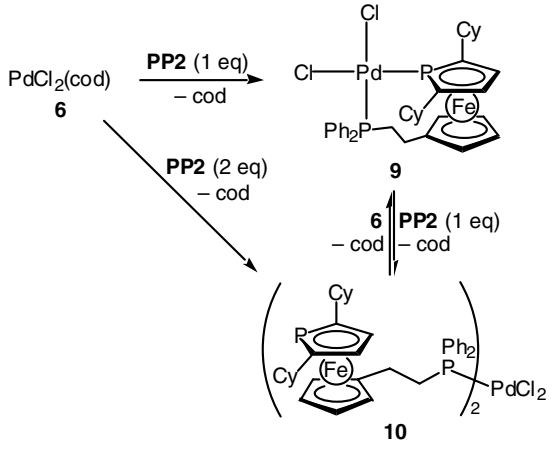

Scheme 3.

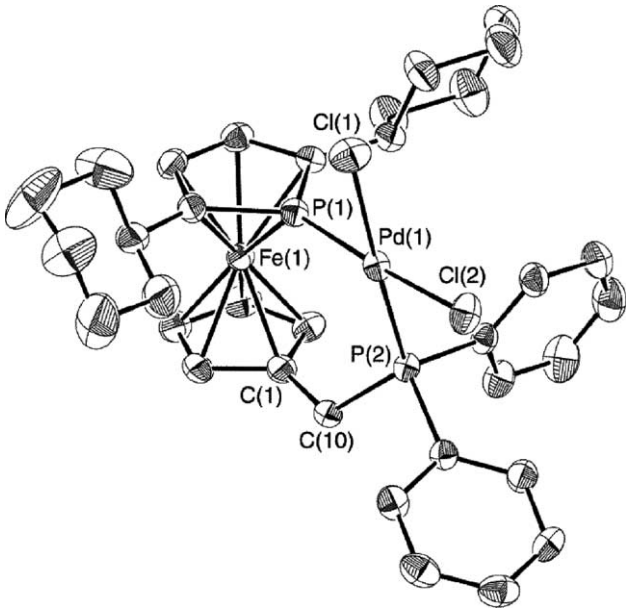

Fig. 3. ORTEP of $PdCl_2$(**PP1**) · CH_2Cl_2 (**7** · CH_2Cl_2) with 50% thermal ellipsoids. All hydrogen atoms and co-crystallized CH_2Cl_2 are omitted for clarity.

the Ph_2P-part of the extra **PP2** to form a bis(phosphino-phosphaferrocene) complex **10** in which **PP2** coordinates as a monodentate ligand. While the chelate complex **9** was an only species detected in the ^{31}P NMR spectrum with a **PP2/6** = 1/1 molar ratio, the complex **10** with the monodentate **PP2** was a sole detectable product from the reaction of **PP2** and **6** with a 2:1 molar ratio. When **PP2** coordinates to a $PdCl_2$ fragment, chelate effect is negligibly weak. This is in clear contrast to the coordination behavior of **PP1** mentioned above. Note that the complex **10** was yielded as a single isomer. [1]

3.3. X-ray crystal structures of dichloropalladium complexes

The complex **7** was readily and quantitatively obtained from an equimolar mixture of **6** and **PP1** in dichloromethane. Recrystallization from CH_2Cl_2–pentane gave prismatic crystals and the structure was clarified by X-ray single-crystal structure determination (Fig. 3). Selected crystallographic data are summarized in Table 1 and selected bond lengths and angles are listed in Table 2. It reveals that the crystal contains a solvent molecule (CH_2Cl_2) per formula unit (the co-crystallized dichloromethane molecule is omitted from the ORTEP drawing for clarity), though no interaction is observed between the complex and the co-crystallized dichloromethane. A

[1] Although a structure of the complex **10** was uncertain, it is tentatively assigned as a *cis*-complex which is electronically more stable than the *trans*-counterpart.

Table 1
Crystallographic data for complexes **7** and **9**

	7	**9**
Formula	$C_{34}H_{40}Cl_2FeP_2Pd \cdot CH_2Cl_2$	$C_{35}H_{42}Cl_2FeP_2Pd$
Formula weight	828.72	757.82
Color, habit	orange, prismatic	brown, prismatic
Crystal size (mm)	$0.25 \times 0.20 \times 0.10$	$0.40 \times 0.13 \times 0.13$
Crystal system	monoclinic	monoclinic
Space group	P_1/a (#14)	P_1/a (#14)
a (Å)	14.0246(7)	14.4360(4)
b (Å)	18.7392(9)	12.9326(4)
c (Å)	14.2839(9)	19.0257(5)
β (°)	105.668(2)	110.382(1)
V (Å^3)	3614.5(3)	3329.6(2)
Z	4	4
D_{calc} (g cm^{-3})	1.523	1.512
μ (cm^{-1})	1.306	1.256
Radiation type	Mo Kα	Mo Kα
Wavelength (Å)	0.7107	0.7107
T (K)	298.2	298.2
$2\theta_{max}$ (°)	55	55
Number of reflections collected	8099	7626
Unique	4971	5799
Parameters	388	406
Refinements on	F^2	F^2
$R[F^2 > 2.0\sigma(F^2)]$	0.0440	0.0416
$R_w[F^2 > 2.0\sigma(F^2)]$	0.0547	0.0578
Goodness-of-fit	1.249	1.577
Residual ρ (e Å^{-3})	+0.91, −0.67	+0.69, −0.70

Table 2
Selected bond distances (Å) and angles (°) for **7**

Bond distances			
Pd(1)–Cl(1)	2.358(2)	C(1)–C(10)	1.502(7)
Pd(1)–Cl(2)	2.322(2)	P(2)–C(10)	1.843(5)
Pd(1)–P(1)	2.226(2)	Fe(1)–P(1)	2.214(2)
Pd(1)–P(2)	2.269(1)	Fe(1)–C(1)	2.048(5)
Bond angles			
Cl(1)–Pd(1)–Cl(2)	91.83(6)	P(1)–Fe(1)–C(1)	100.9(2)
Cl(1)–Pd(1)–P(1)	85.48(6)	Pd(1)–P(1)–Fe(1)	132.82(7)
Cl(1)–Pd(1)–P(2)	176.44(6)	Fe(1)–C(1)–C(10)	130.6(4)
Cl(2)–Pd(1)–P(1)	176.45(6)	P(2)–C(10)–C(1)	121.7(3)
Cl(2)–Pd(1)–P(2)	89.20(5)	Pd(1)–P(2)–C(10)	119.2(2)
P(1)–Pd(1)–P(2)	93.35(5)		

solvent-free sample was obtained by prolonged evacuation under high-vacuum at 50 °C. The angle of P(1)–Pd(1)–P(2) is 93.35(5)°, while that of Cl(1)–Pd(1)–Cl(2) is 91.83(6)°. The bite angle of the coordinating **PP1** in **7** was unremarkable: it is in the typical range for dichloropalladium(II) complexes bearing chelating bisphosphine ligands [11]. The geometry around the Pd center is slightly distorted square planar, the sum of four angles at Pd(1) involving Cl(1), Cl(2), P(1), and P(2) being 359.9(2)°. The Pd–P distances and the Pd–Cl distances are in the typical range for $PdCl_2$(P–P) complexes.

An analogous complex with **PP2**, $PdCl_2$(**PP2**) (**9**) was prepared from **6** in a similar manner and its solid state structure was determined by X-ray crystallography

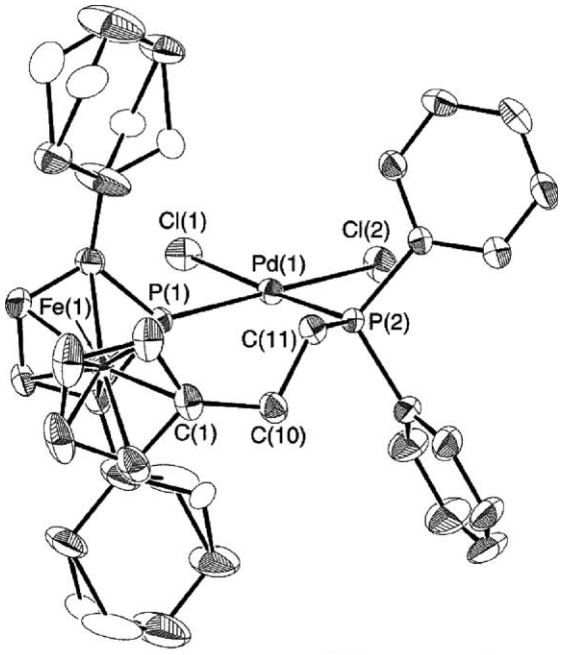

Fig. 4. ORTEP of $PdCl_2$(**PP2**) (**9**) with 50% thermal ellipsoids. All hydrogen atoms are omitted for clarity.

(Fig. 4, Tables 1 and 3). Unlike the complex **7**, the crystals of **9** have no co-crystallized solvent. Some disorders are detected in both of the cyclohexyl groups. Although small distortion of the bond angles around the palladium center is observed in **9**, Pd(1), P(1), P(2), Cl(1), and Cl(2) are located on the same plane and sum of the angles between the adjacent coordination sites is 360.1(2)°. The P(1)–Pd(1)–P(2) bite angle in the complex **9** is significantly larger than that in **7**, being 96.59(4)°. The weak chelate effect of **PP2** could be attributed to the large bite angle of the chelating ligand.

3.4. Comparison between *1*, *PP1*, and *PP2*

Comparison of the overall coordination behavior of **PP1** and **PP2** indicates that elongation of the bridging unit between C_5H_4 and PPh_2 in the phosphino-phos-

Table 3
Selected bond distances (Å) and angles (°) for **9**

Bond distances			
Pd(1)–Cl(1)	2.369(1)	C(1)–C(10)	1.496(7)
Pd(1)–Cl(2)	2.328(1)	C(10)–C(11)	1.556(6)
Pd(1)–P(1)	2.223(1)	Fe(1)–P(1)	2.215(1)
Pd(1)–P(2)	2.261(1)	Fe(1)–C(1)	2.036(4)
P(2)–C(11)	1.833(4)		
Bond angles			
Cl(1)–Pd(1)–Cl(2)	92.83(5)	P(1)–Fe(1)–C(1)	106.4(1)
Cl(1)–Pd(1)–P(1)	83.02(4)	Pd(1)–P(1)–Fe(1)	148.95(5)
Cl(1)–Pd(1)–P(2)	176.58(4)	Fe(1)–C(1)–C(10)	125.6(3)
Cl(2)–Pd(1)–P(1)	175.09(5)	C(1)–C(10)–C(11)	115.0(4)
Cl(2)–Pd(1)–P(2)	87.70(5)	P(2)–C(11)–C(10)	117.8(3)
P(1)–Pd(1)–P(2)	96.59(4)	Pd(1)–P(2)–C(11)	118.8(1)

phaferrocenes diminishes their chelation ability. As shown in the crystal structures, the size of the chelate ring (i.e., the P–Pd–P angle) in **7** is nearly ideal for the square planar Pd^{II} center, while the ethylene unit bridging the PPh_2 and the phosphaferrocene in **PP2** causes certain deviations from an idealized geometry in the square planar complex **9**. The latter may be the main reason for the weaker chelation ability of **PP2**. Because of the structural similarity between **1** and **PP1**, a possible chelate ring strain in **1** could be excluded as a main factor for the weak chelate effect in **1**.

Difference of the coordination behavior between **1** and **PP1** is distinctive, although their structural differences are very minor. Because the electronic effects from (–)-menthyl groups in **1** and from cyclohexyl groups in **PP1** are assumed to be nearly identical, the difference of their complexation behavior to Pd^{II} could be ascribed to the difference of their steric characteristics. In other words, the bulky (–)-menthyl groups in **1** cause steric congestion at the phosphorus atom in the phospholyl group. This weakens the coordination ability of the phosphaferrocene moiety in **1**, and thus chelate effect in the ligand **1** becomes weaker.

From this study, it is concluded that steric bulk of (–)-menthyl groups in **1** is the main factor of the weak chelate coordination of **1**.

4. Supplementary material

Complete crystallographic data for **7** and **9** in CIF format.

Acknowledgements

This work was partially supported by a Grant-in-Aid for Scientific Research on Priority Areas (No. 15036202, "Reaction Control of Dynamic Complexes") from the Ministry of Education, Culture, Sports, Science and Technology, Japan.

References

[1] (a) M. Ogasawara, K. Yoshida, T. Hayashi, Organometallics 20 (2001) 3913;
(b) M. Ogasawara, K. Yoshida, T. Hayashi, Organometallics 20 (2001) 1014.
[2] (a) C. Ganter, L. Brassat, B. Ganter, Chem. Ber./Recueil 130 (1997) 1771;
(b) L. Brassa, B. Ganter, C. Ganter, Chem. Eur. J. 4 (1998) 1163.
[3] (a) S. Qiao, G.C. Fu, J. Org. Chem. 63 (1998) 4168;
(b) K. Tanaka, S. Qiao, M. Tobisu, M.M.-C. Lo, G.C. Fu, J. Am. Chem. Soc. 122 (2000) 9870;
(c) K. Tanaka, G.C. Fu, J. Org. Chem. 66 (2001) 8177.
[4] (a) J. Fischer, A. Mitschler, L. Ricard, F. Mathey, J. Chem. Soc., Dalton Trans. (1980) 2522;
(b) F. Mathey, J. Fischer, J.H. Nelson, Struct. Bonding 55 (1983) 153;
(c) F. Mathey, J. Organomet. Chem. 400 (1990) 149;
(d) F. Mathey, Coord. Chem. Rev. 137 (1994) 1.
[5] C.-F. Shu, F.C. Anson, J. Phys. Chem. 94 (1990) 8345.
[6] M. Ogasawara, T. Nagano, K. Yoshida, T. Hayashi, Organometallics 21 (2002) 3062.
[7] D. Drew, J.R. Doyle, Inorg. Synth. 13 (1972) 52.
[8] R.M.G. Robert, A.S. Wells, Inorg. Chim. Acta 112 (1986) 171.
[9] D. Astruc, Tetrahedron 39 (1983) 4027.
[10] J.P. Collman, L.S. Hegedus, J.R. Norton, R.G. Finke, Principles and Applications of Organotransition Metal Chemistry, University Science Books, Mill Valley, CA, 1987.
[11] (a) W.L. Steffen, G.J. Palenik, Inorg. Chem. 15 (1976) 2432;
(b) V.D. Makhaev, Z.M. Dzhabieva, S.V. Konovalikhin, O.A. D'yachenko, G.P. Belov, Russ. J. Coord. Chem. 22 (1996) 563;
(c) T. Hayashi, M. Konishi, Y. Kobori, M. Kumada, T. Higuchi, K. Hirotsu, J. Am. Chem. Soc. 106 (1984) 158;
(d) F. Ozawa, A. Kubo, Y. Matsumoto, T. Hayashi, Organometallics 12 (1993) 4188;
(e) M. Ogasawara, K. Yoshida, T. Hayashi, Organometallics 19 (2000) 1567.